Article

Generation of Superparamagnetic Liposomes Revealed as Highly Efficient MRI Contrast Agents for in Vivo Imaging

Marie-Sophie Martina, Jean-Paul Fortin, Christine Mnager, Olivier Clment, Gillian Barratt, Ccile Grabielle-Madelmont, Florence Gazeau, Valrie Cabuil, and Sylviane Lesieur

J. Am. Chem. Soc., **2005**, 127 (30), 10676-10685• DOI: 10.1021/ja0516460 • Publication Date (Web): 08 July 2005

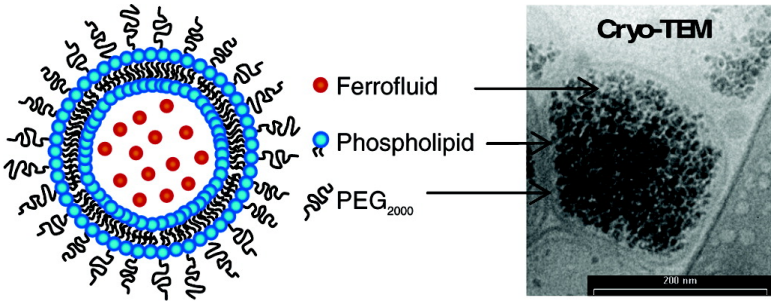

More About This Article

Additional resources and features associated with this article are available within the HTML version:

- Supporting Information
- Links to the 36 articles that cite this article, as of the time of this article download
- Access to high resolution figures
- Links to articles and content related to this article
- Copyright permission to reproduce figures and/or text from this article

View the Full Text HTML

J|A|C|S
ARTICLES
Published on Web 07/08/2005

Generation of Superparamagnetic Liposomes Revealed as Highly Efficient MRI Contrast Agents for in Vivo Imaging

Marie-Sophie Martina,[†] Jean-Paul Fortin,[§,||] Christine Ménager,[‡] Olivier Clément,[§] Gillian Barratt,[†] Cécile Grabielle-Madelmont,[†] Florence Gazeau,[||] Valérie Cabuil,[‡] and Sylviane Lesieur*[,†]

Contribution from the Laboratoire de Physico-Chimie des Systèmes Polyphasés, UMR CNRS 8612, Université Paris-Sud, Faculté de Pharmacie, 5 rue Jean-Baptiste Clément, F-92296 Châtenay-Malabry Cedex, France, Laboratoire des Liquides Ioniques et Interfaces Chargés, UMR CNRS 7612, Université Pierre et Marie Curie, case 63, 4 place Jussieu, F-75252 Paris Cedex, France, Laboratoire de Recherche en Imagerie, INSERM U494, Faculté de Médecine Necker Enfants Malades, Paris, France, and Laboratoire Matière et Systèmes Complexes, UMR 7057, Université Paris 7, 2 place Jussieu − 75251 Paris Cedex 05, France

Received March 15, 2005; E-mail: sylviane.lesieur@cep.u-psud.fr

Abstract: Maghemite (γ-Fe_2O_3) nanocrystals stable at neutral pH and in isotonic aqueous media were synthesized and encapsulated within large unilamellar vesicles of egg phosphatidylcholine (EPC) and distearoyl-SN-glycero-3-phosphoethanolamine-*N*-[methoxy(poly(ethylene glycol))-2000] (DSPE-PEG_{2000}, 5 mol %), formed by film hydration coupled with sequential extrusion. The nonentrapped particles were removed by flash gel exclusion chromatography. The magnetic-fluid-loaded liposomes (MFLs) were homogeneous in size (195 ± 33 hydrodynamic diameters from quasi-elastic light scattering). Iron loading was varied from 35 up to 167 Fe(III)/lipid mol %. Physical and superparamagnetic characteristics of the iron oxide particles were preserved after liposome encapsulation as shown by cryogenic transmission electron microscopy and magnetization curve recording. In biological media, MFLs were highly stable and avoided ferrofluid flocculation while being nontoxic toward the J774 macrophage cell line. Moreover, steric stabilization ensured by PEG-surface-grafting significantly reduced liposome association with the macrophages. The ratios of the transversal (r_2) and longitudinal (r_1) magnetic resonance (MR) relaxivities of water protons in MFL dispersions ($6 < r_2/r_1 < 18$) ranked them among the best T_2 contrast agents, the higher iron loading the better the T_2 contrast enhancement. Magnetophoresis demonstrated the possible guidance of MFLs by applying a magnetic field gradient. Mouse MR imaging assessed MFLs efficiency as contrast agents in vivo: MR angiography performed 24 h after intravenous injection of the contrast agent provided the first direct evidence of the stealthiness of PEG-ylated magnetic-fluid-loaded liposomes.

Introduction

Magnetic resonance imaging (MRI) ranks among the best noninvasive methodologies today available in clinical medicine for assessing anatomy and function of tissues.[1,2] Its main advantages are that it allows rapid in vivo acquisition of images and, under specific conditions, it makes possible imaging at cell resolution. MRI is based upon the property of hydrogen nuclei of water to align with and precess around an applied static magnetic field. The precessing hydrogen nuclei can be perturbed by radio frequency pulses, and the processes through which they return to their original aligned state can be exploited to give an image. The contrast comes from local differences in spin relaxation kinetics along the longitudinal (spin−lattice relaxation time T_1) and transverse (spin−spin relaxation time T_2) planes of the main magnetic field applied to the specimen. On this basis, endogenous contrast depends on the chemical and physical nature of the tissues and often arises from local variation in the proton density (water concentration). Otherwise, the use of exogenous substances or contrast agents that alter signal intensity by selectively shortening the hydrogen relaxation times of the tissues becomes essential to improve sensitivity and specificity of MRI.[3]

For the last 20 years, the chemistry of contrast agents for use in vivo has been significantly developed. Paramagnetic metallochelates, principally gadolinium derivatives, have received particular attention. They typically behave as T_1 contrast agents, which cause positive contrast enhancement and provide brighter images where they are accumulated. Besides, particle systems based on superparamagnetic iron oxide (SPIO) or ultra small paramagnetic iron oxide (USPIO) have emerged as T_2 contrast agents, which permit negative contrast enhancement and thus darker images of the regions of interest. Although

[†] Université Paris-Sud.
[‡] Université Pierre et Marie Curie.
[§] Faculté de Médecine Necker Enfants Malades.
[||] Université Paris 7.

(1) Bulte, J. W. M.; van Zijl, P. C. M.; Mori, S. *Trends Biotechnol.* **2002**, *20*, S24−S28.
(2) Pautler, R. G.; Fraser, S. E. *Curr. Opin. Immunol.* **2003**, *15*, 385−392.
(3) Tilcock, C. *Adv. Drug Delivery Rev.* **1999**, *37*, 33−51.

10.1021/ja0516460 CCC: $30.25

progress has been made in both the preparation of these systems and their targeting to specific cells or tissues, their administration and distribution within the organism and the possible role of delivery systems remains an active research area.[4−7] The first concern is to reduce both their instability in biological media and the concentration necessary for efficient functioning, thus minimizing toxic effects and cost while maintaining high-resolution contrast. The second issue is the targeting of the tissues to be visualized by the contrast agents. Different strategies such as binding of proteins or sequestration within dendrimer for metallochelates[8,9] or polymer coating for SPIOs[10,11] have undoubtedly proved their worth. More than 10 contrast agents of this type are commercially available to date.[12] Another strategy that consists of entrapping MRI contrast agents into liposomes has also been investigated,[3,13] but to a lesser extent. This is surprising if we consider the considerable potential advantages of liposome encapsulation, that is, avoiding local dilution of the contrast agents and limiting their interactions with biological media into which they are administered. Lipid vesicles are highly compatible with biological membranes in both composition and structure, and thus their utility as drug delivery systems is well established.[14−17] In this respect, liposomes allow the combination of diagnosis and therapeutics by encapsulating a MRI contrast agent and a drug together.

Recently, we proposed a reliable method for producing large unilamellar liposomes entrapping monodisperse nanocrystals of maghemite (γ-Fe_2O_3) with the aim of demonstrating the surfactant-induced formation of transient pores in lipid bilayers.[18] Our purpose here is to evaluate these magnetic-fluid-loaded liposomes as MRI contrast agents for use in vivo. Accordingly, the synthesis of the maghemite colloidal suspension was revised to yield a ferrofluid stable in physiological conditions while still behaving as a T_2 contrast agent.[11] The procedure of liposome preparation was also improved to increase final vesicle concentration and ferrofluid encapsulation rates. Because these liposomes were intended as carriers for systemic administration, it was necessary to maximize their biological half-life. On the basis of previous eloquent studies, this was resolved by introducing poly(ethylene glycol)-grafted lipids into the vesicle bilayer.[19−23]

This Article describes the physical and biological properties of the magnetoliposomes prepared according to this strategy. Complementary techniques were employed to characterize their structure and magnetic behavior, such as electron microscopy, quasi-elastic light scattering, relaxometry, and magnetophoresis. The ability of the liposomes to escape uptake by the mononuclear phagocyte system was assessed in vitro by examining interactions with a model macrophage cell line, J774. Prolonged circulation in blood and magnetic resonance contrast efficiency were examined in vivo by performing angiographic MRI in mice.

Materials and Methods

Materials. Chloroform solutions of egg-yolk L-α-phosphatidylcholine (EPC, M = 760.08) and 1.2-diacyl-SN-glycero-3-phosphoethanolamine-*N*-[methoxy(poly(ethylene glycol))-2000] (DSPE-PEG_{2000}, M = 2805.54) were purchased from Avanti Polar Lipids (Alabaster, AL). Sodium chloride, sodium citrate, Triton X100, *n*-octyl-β,D-glucopyranoside (OG), *N*-[2-hydroxyethyl]piperazine-*N*′-[2-ethanesulfonic acid] (HEPES), and dimethylthiazolyldiphenyl-tetrazolium bromide (MTT) were provided by Sigma (St Louis, MO).

Unless otherwise stated, the buffer used was 108 mM NaCl, 20 mM sodium citrate, 10 mM HEPES, pH 7.4, and 285 mOsm (measured with a cryoscopic micro-osmometer, Bioblock Scientific, France).

Synthesis of Maghemite Nanoparticles. According to a procedure already described, superparamagnetic Fe_3O_4 (magnetite) nanocrystals were prepared by alkaline coprecipitation of $FeCl_2$ and $FeCl_3$ salts.[18,24] Monodisperse γ-Fe_2O_3 (maghemite) nanocrystals were synthesized by oxidizing magnetite (1.3 mol) into 1 L of nitric acid 2 N containing 1.3 mol of iron nitrate under boiling. After being decantation-sieved, the maghemite particles were heated at 80 °C for 30 min in water supplemented with 70 g of sodium citrate before being precipitated in acetone at 25 °C, filtered and suspended in 23 mM aqueous sodium citrate by conductivity-controlled dialysis. Final adjustment of both aqueous medium (108 mM NaCl, 20 mM sodium citrate, 10 mM HEPES, pH 7.4 buffer) and maghemite concentration was performed by ultrafiltration. A 12-mL aliquot of the colloidal particle suspension was centrifuged in a MACROSEP filter, cutoff 50 kD (Fisher Scientific Labosi, France) at 12 000*g* for 30 min. Next, 10 mL buffer was added into the filter before a second similar centrifugation. Twice-centrifuged particles were diluted again with buffer to obtain the desired Fe(III) concentration in the 0.7−5.4 M range. Final iron contents were checked by flame spectrometry. The recovered magnetic fluid was ready to use and stable at room temperature for at least 1 year.

Liposome Preparation. Magnetic-fluid-loaded liposomes (MFLs) were prepared by the thin film hydration method coupled with sequential extrusion. Aliquots of EPC or DSPE-PEG_{2000} supplied as chloroform solutions were placed into vials to form either EPC (100 mol %) or EPC:DSPE-PEG_{2000} (95:5 mol %) films by removing chloroform under a nitrogen stream followed by evaporation under vacuum for 12 h. Lipid contents were determined by weight (precision, 5×10^{-5} g). Dry films were hydrated by adding equal volumes of the suspension of maghemite particles to be loaded and buffer to get a total lipid concentration of 20 mM. Various maghemite concentrations were used to obtain different final concentrations in the liposomes. Dispersions were homogenized with vortex mixing and extruded under nitrogen pressure (<10 bar) at 25 °C through polycarbonate filters (PORETICS, Osmotics, Livermore, USA) of decreasing pore diameters 0.8 μm/0.4 μm/0.2 μm (2 passages through each).

Nonentrapped maghemite particles were removed by gel exclusion chromatography (GEC) performed with a 0.4 × 5.8 cm Sephacryl S1000 superfine (Pharmacia) microcolumn (TERUMO 1 mL-syringe)

(4) Torchilin, V. P. *Adv. Drug Delivery Rev.* **1997**, *24*, 301−313.
(5) Bogdanov, A. A.; Lewin, M.; Weissleder, R. *Adv. Drug Delivery Rev.* **1999**, *37*, 279−293.
(6) Okuhata, Y. *Adv. Drug Delivery Rev.* **1999**, *37*, 121−137.
(7) Shinkai, M. *J. Biosci. Bioeng.* **2002**, *94*, 606−613.
(8) Matthews, S. E.; Pouton, C. W.; Threadgill, M. D. *Adv. Drug Delivery Rev.* **1996**, *18*, 219−267.
(9) Torchilin, V. P. *Eur. J. Pharm. Sci.* **2000**, *11 Suppl 2*, S81−91.
(10) Kellar, K. E.; Fujii, D. K.; Gunther, W. H.; Briley-Saebo, K.; Spiller, M.; Koenig, S. H. *Magma* **1999**, *8*, 207−213.
(11) Weissleder, R.; Bogdanov, A.; Neuwelt, E. A.; Papisov, M. *Adv. Drug Delivery Rev.* **1995**, *16*, 321−334.
(12) Weinmann, H. J.; Ebert, W.; Misselwitz, B.; Schmitt-Willich, H. *Eur. J. Radiol.* **2003**, *46*, 33−44.
(13) Torchilin, V. P. *Curr. Pharm. Biotechnol.* **2000**, *1*, 183−215.
(14) Woodle, M. C. *Adv. Drug Delivery Rev.* **1995**, *16*, 249−265.
(15) Lasic, D. D.; Papahadjopoulos, D. *Curr. Opin. Solid State Mater. Sci.* **1996**, *1*, 392−400.
(16) Marjan, J. M.; Allen, T. M. *Biotechnol. Adv.* **1996**, *14*, 151−175.
(17) Maruyama, K.; Ishida, O.; Takizawa, T.; Moribe, K. *Adv. Drug Delivery Rev.* **1999**, *40*, 89−102.
(18) Lesieur, S.; Grabielle-Madelmont, C.; Menager, C.; Cabuil, V.; Dadhi, D.; Pierrot, P.; Edwards, K. *J. Am. Chem. Soc.* **2003**, *125*, 5266−5267.
(19) Gregoriadis, G.; Florence, A. T. *Cancer Cells* **1991**, *3*, 144−146.
(20) Needham, D.; Hristova, K.; McIntosh, T. J.; Dewhirst, M.; Wu, N.; Lasic, D. D. *J. Liposome Res.* **1992**, *2*, 411−430.
(21) Allen, T. M.; Hansen, C. B.; de Menezes, D. E. L. *Adv. Drug Delivery Rev.* **1995**, *16*, 267−284.
(22) Beugin, S.; Edwards, K.; Karlsson, G.; Ollivon, M.; Lesieur, S. *Biophys. J.* **1998**, *74*, 3198−3210.
(23) Woodle, M. C. *Adv. Drug Delivery Rev.* **1998**, *32*, 139−152.
(24) Massart, R. 4329241: U.S., 1982.

saturated with lipids before sample elution. The eluent was the buffer used for liposome preparation. Under these conditions, 200 μL of liposome dispersion could be purified without loss or dilution of material. Fraction collection was performed directly into the optical cells used for quasi-elastic light scattering analysis, and collected volumes were determined by weight. Iron loading was measured independently by flame spectrometry and electron paramagnetic resonance (EPR) using an experimental device previously described.[25] The final lipid concentration was determined by an enzymatic assay (Phospholipides Enzymatiques PAP 150, Biomérieux, France). A maximum variation of $\pm$0.5 mM lipids was found between the liposome preparation before extrusion (20 mM concentration by weight) and the extruded liposome preparation recovered after chromatography.

The encapsulation efficiency of the liposomes is the ratio of the number of maghemite particles contained in the internal volume of the final liposomes after GEC purification to the total number of maghemite particles contained in the initial liposome dispersion before GEC. Maghemite contents were determined by UV−visible absorption in the 400−600 nm wavelength range. Spectra were recorded with a double-beam spectrophotometer (Lambda 2, Perkin-Elmer). Before analysis, the initial and GEC-purified liposomes were totally solubilized into mixed micelles to completely release the entrapped particles and to avoid interference from scattering of light by vesicles: 2 mL of a 100 mM OG solution in buffer was added to 200 μL of each. The encapsulation efficiency was given by the ratio of the optical densities at 570 nm of the GEC-purified and initial liposomes.

The stability study was performed by diluting initial liposome preparations (25 μL, 20 mM lipids) in different media (975 μL, 0.5 mM final lipids). The aspect as well as hydrodynamic diameter of the particles were followed over a period of 3 months.

Quasi-elastic Light Scattering (QELS). Hydrodynamic diameters of maghemite particles and liposomes were determined by QELS with a Nanosizer (N4 MD, Coultronics), at 25 °C, 90° scattering angle, and using size distribution processor (SDP) analysis. Just before measurements, the sample were diluted with buffer to optimize the response of the apparatus, that is, typically to Fe(III) and total lipid concentrations close to 10^{-2} M and 0.5 mM for free magnetic fluid and liposomes, respectively. Mean hydrodynamic diameters d_h were calculated from the mean translational diffusion coefficient D of the particles according to the Stokes−Einstein law for spherical and noninteracting particles: $d_h = k_B T/3\pi\eta D$ (k_B, Boltzmann constant; η dispersant viscosity).

Confocal Microscopy. A mixture of PEG-ylated MFL (0.67 mM lipids) and calibrated fluorescent microspheres (Tetraspeck 0.2 μm, 515 nm emission wavelength, Molecular Probes, Eugene, Oregon, USA) were examined by confocal laser scanning microscope CLSM 510 (Zeiss, Germany), coupled to LSM 5 Image Brother (Zeiss, Germany). Fluorescent images were acquired with an air-cooled ion laser at 488 nm. Both Nomarski and fluorescent images were performed using a Plan Apochromat 63x/1.4NO oil objective lens.

Cryogenic Transmission Electron Microscopy (Cryo-TEM). Structures of magnetoliposomes were characterized by cryo-TEM. The liposomes, prepared at 20 mM lipids and containing 18 mM of iron, were diluted at 1 mM lipids with buffer before observation. The specimens were rapidly frozen by plunge-freezing in liquid ethane cooled by liquid nitrogen (LEICA EM CPC, Wien, Austria). The cryofixed specimens were mounted into a Gatan cryoholder (626 DH cryotransfer specimen holder/Gatan inc., Warrendale, PA) for direct observation at −170 °C in a Leo 912 energy-filtered cryo-TEM operating at 120 kV with a LaB6 filament. Images were recorded with a cooled slow-scan CCD camera (Proscan, Penzing, Germany) equipped with a 1024 × 1024 pixel-sized chip and operating in a 14-bit mode. Acquisition was accomplished with the ESIvision program (versions 3. 0 Soft-Imaging Software, SIS, GmbH, D-48153 Münster).

Magnetization Measurements. The magnetization curves of the maghemite particles suspension were determined using a vibrating magnetometer.[26,27] The shape of the magnetization curves was fitted according to Langevin's law, which gives the relationship between the magnetization m of the magnetic particles per unit volume as a function of their volume fraction Φ and diameter d when they are submitted to a magnetic field B: $m/m_s = \Phi(\coth(\xi) - 1/\xi)$ with $\xi = m_s\pi d^3 B/6k_B T$ (k_B, Boltzmann constant; $m_s = 3.1 \times 10^5$ A m^{-1}, saturation magnetization of maghemite).

Relaxometry. Relaxation times were measured at 0.47 T (20 MHz proton Larmor frequency) and 37 °C using a Minispec PC120 spectrometer (Brucker, France). T_1 relaxation time was calculated from the inversion−recovery sequence, with 15 data points and 3 acquisitions for each measurement. T_2 relaxation time was obtained from a Carr−Purcell Meiboom Gill (CPMG) spin−echo pulse sequence (interpulses delay of 2 ms, 100 data points, 3 acquisitions). T_1 and T_2 were determined three times for each sample with standard deviations of 2% and 5%, respectively. Samples were diluted in buffer, and the relative error determined from two independent sample series was found less than 5% for both relaxation times.

Magnetophoresis. Liposome magnetophoresis was performed by using an experimental device already described in details.[25] A droplet of liposome preparation was set down onto a glass slide previously treated with dimethyldichlorosilane to prevent liposomes from adhering to the glass. Liposomes were then induced to migrate by applying a 0.36 T magnetic field with a collinear field gradient of 36 T/m. Their movement was recorded by a video system adapted to an inverted microscope.

Cell Culture and Preparation. The J774 A1 murine macrophage cell line (ECACC catalog number 91051511) was maintained as an adherent culture and was grown as a monolayer in a humidified incubator (95% air; 5% CO_2) at 37 °C in 75-cm^2-flasks (Nunc) containing RPMI 1640 Glutamax-I medium (GIBCO) supplemented with 10% (v/v) heat-inactivated foetal calf serum (FCS, GIBCO), 100 IU/mL penicillin, and 100 IU/mL streptomycin (GIBCO). For experiments, the cells were detached mechanically and adjusted to the required concentration of viable cells, by counting in a hemocytometer in the presence of trypan blue. Under our culture conditions, the cell number increased by a factor of 2.5 $\pm$ 0.5 during a 24-h incubation.

Cytotoxicity. Cells were plated in 96-well plates (COSTAR, France) at 10^5 per mL (200 μL per well) 24 h before adding either maghemite particles or liposome preparations at the desired concentrations (from 2×10^{-3} to 2×10^{-8} mol of iron/L per well). After 1-, 4-, or 24-h incubations, the supernatant was removed and adherent cells were washed three times with RPMI. Cell viability was then estimated using the MTT conversion test.[28] Absorption at 570 nm was measured on a Labsystems Multiskan MS spectrometer. Each result was the average of 6 wells, and 100% viability was determined from untreated cells deposited on each 96-well plate.

Association with Cells. Cells were plated in 6-well plates (COSTAR, France) at 2.5×10^6 per mL (2 mL per well) 2 h before incubation (1 or 4 h) with magnetic-fluid-loaded liposomes at different Fe(III) concentrations. Iron capture was determined after removing the supernatant and twice washing the cells with RPMI. The remaining cells and cell-associated liposomes were scraped off, solubilized in a 0.1% (w/v) Triton-X100 distilled water solution (2 × 0.85 mL per well), and maghemite was quantified by its absorption at 492 nm (Perkin-Elmer Lamda 2 double-beam spectrophotometer). After lysate pooling, 100 μL aliquots were analyzed for protein content by the BIO-RAD Protein Assay using bovine serum albumin as standard. Each experiment was repeated three times.

Magnetic Resonance Imaging (MRI) in Vivo. Animal experiments were performed in accordance with the INSERM animal protection guidelines and approved by local governmental authorities. Experiments

(25) Wilhelm, C.; Gazeau, F.; Bacri, J. C. *Eur. Biophys. J.* **2002**, *31*, 118−125.
(26) Foner, S.; McNiff, E. J. *Rev. Sci. Instrum.* **1968**, *39*, 171−179.
(27) Bacri, J. C.; Perzynski, R.; Salin, D. *J. Magn. Magn. Mater.* **1986**, *62*, 36−46.
(28) Mosmann, T. *J. Immunol. Methods* **1983**, *65*, 55−63.

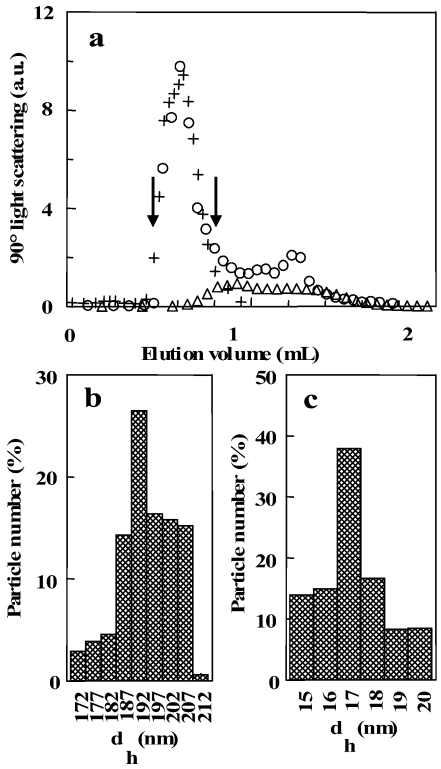

Figure 1. Purification of magnetic-fluid-loaded liposomes (MFL) by gel exclusion chromatography. Elution profiles after separately injected ferrofluid (△), unloaded EPC:DSPE-PEG_{2000} (95:5 mol %) liposomes (+), and EPC:DSPE-PEG_{2000} (95:5 mol %) MFL (○). Sample loading: 200 μL. Arrows delimit the 200 μL-fraction containing pure MFL. (b) EPC:DSPE-PEG_{2000} (95:5 mol %) MFL and (c) ferrofluid size distributions from QELS measurements of 20 μL GEC fractions collected on-line at the end of the column.

were carried out on male Swiss Nude mice (Iffa Credo, L'Arbresle, France), weighing between 25 and 31 g. Animals were anaesthetized by intraperitoneal injection of 0.1 mL/10 g ROMPUM 2% IMALGENE 500 (4:1 v/v) solution. During anaesthesia, mouse body temperature was kept at physiological level using a heating lamp. Magnetic material (200 μL; 0.11 mg Fe(III)) was injected into the caudal vein. Control animals were injected with physiological serum.

MRI experiments in vivo were conducted on a clinical 1.5 T MR imager (Signa 1.5 T, General Electric, Milwaukee, WI). Animals were placed into a custom-built 3-cm diameter Helmhotz coil used for emission and reception. T_1-weighted spin−echo (SE) sequences (TR = 500 ms; TE = 11 ms) and T_1-weighted 3D spoil gradient echo (SPGR) sequences (TR = 37.4 ms; TE = 8.6 ms) were carried out at different times after MFL injection. Regions of interest (ROI) were defined by using Scion image software (Scion Corp., NIH, USA). The signal intensity of the ROI was normalized by the signal from an oil phantom in a tube placed next to the mouse into the coil. Enhancement (ENH) between normalized signals of injected animals (SI) and controls (SI_{ref}), respectively, was calculated in each ROI as: $ENH\ (\%) = (SI - SI_{ref}) \times 100/SI_{ref}$.

Results

Characterization of the Maghemite-Loaded Liposomes. Structure and Stability. Both conventional (100% EPC) and poly(ethylene glycol)-grafted (95/5 mol %) liposomes containing maghemite nanocrystals were prepared in the same way. Once formation of magnetic-fluid-loaded liposomes (MFLs) had been achieved, the nonencapsulated maghemite was removed by low-pressure gel exclusion chromatography in conditions that avoided lipid dilution. Figure 1 shows the elution profiles recorded after separate loading of free maghemite nanocrystals, nonloaded liposomes, and MFLs preparation just after extrusion. The GEC peaks of the liposomes and particles clearly presented no overlapping, showing that finally recovered MFLs were completely free of contaminating external maghemite. Moreover, the profiles in Figure 1 show that 96 ± 4% of liposomes were eluted within a 200 μL volume equal to the volume loaded onto the column (200 μL). Consequently, the 200 μL fraction collected from the void volume of the column (500 μL) provided liposomes at a lipid concentration very close to that of the initial preparation. This was confirmed independently by phospholipid assay.

Whatever the initial iron content of the magnetic fluid to be encapsulated, both conventional and PEG-ylated liposomes showed equivalent encapsulation efficiency of 1.8 ± 0.2 Fe-(III) mol %. This corresponds to nearly two maghemite particles encapsulated per 100 maghemite particles initially contained in the magnetic fluid used for lipid hydration. Iron loadings from 0.35 mol up to 1.67 mol of iron per mol of lipids (20 mM total concentration) were obtained by varying the Fe(III) content of the initial maghemite colloidal suspension from 1 to 5.4 M (Table 1). QELS measurements showed that both liposome populations exhibited unimodal distributions centered on 300 nm (conventional liposomes) and from 195 to 200 nm (PEG-ylated liposomes) in hydrodynamic diameters (Table 1). Figure 1b illustrates the narrow size distribution of the PEG-ylated MFLs, which did not exceed 230 nm in hydrodynamic diameter. QELS analysis of collected GEC fractions of the free magnetic fluid confirmed the maghemite particles were quite monodisperse with a hydrodynamic diameter of 17 ± 3 nm (Figure 1c).

Figure 2 exemplifies the images of confocal microscopy recorded from PEG-ylated MFLs, which appeared noninteracting, homogeneous in dimensions and with a diameter twice smaller than up to about the size of calibrated 200 nm beads of a standard latex. One must keep in mind that Nomarski imaging mainly visualizes the internal volume of the liposomes, which are filled with iron oxide of indeed high refractive index as compared to that of the lipid vesicle shell. The internal structure of MFL was characterized by Cryo-TEM. Figure 3 shows a typical picture obtained for the PEG-ylated liposomes. Principally closed unilamellar and maghemite-loaded structures are seen with diameters in the 100−250 nm range. No external ferrofluid can be seen, and entrapped particles presented neither cooperative aggregation nor specific interaction with lipid bilayer. Vesicles appear slightly deformed mainly due to their size being larger than the thickness of the water film in which they were trapped during sample deposition onto the polymer grid.

The physical stability of both conventional and PEG-ylated MFL was evaluated when stored at 6 °C in three different isotonic media: (A) 10 mM HEPES, 108 mM NaCl, 20 mM sodium citrate, pH 7.4, 285 mosmol, (B) 10 mM HEPES, 145 mM NaCl, pH 7.4, 285 mosmol, and (C) cell culture medium RPMI supplemented by 10% (v/v) foetal calf serum and used for the in vitro experiments. QELS measurements as a function of time demonstrated that the diameter remained stable over 3 months at least for both types of liposomes. Partial aggregation could be noticed with time for conventional liposomes with iron loadings higher than 0.5 Fe(III) mol per mol of lipids, but this was reversible upon stirring and did not lead to modification

Table 1. Longitudinal (r_1) and Transversal (r_2) Relaxivities of Magnetic-Fluid-Loaded Liposomes as a Function of Lipid Composition and Iron Loading, as Compared to Values from Free Iron Oxide Particles

system	composition	iron loading[d]	d_h[e]	r_1[f] (mM^{-1} s^{-1})	r_2 (mM^{-1} s^{-1})
ferrofluid[a]	citrate-stabilized maghemite crystals		16 ± 5	36 ± 1	108 ± 5.4
conventional MFL	EPC (100%)	0.35 ± 0.03	300 ± 80	10 ± 0.3	67 ± 3
PEG-ylated MLF	EPC:DSPE-PEG_{2000} (95:5 mol %)	0.53 ± 0.05	200 ± 50	18.6 ± 0.5	116 ± 5.8
id	id	1.35 ± 0.13	202 ± 42	8.5 ± 0.2	124 ± 6.2
id	id	1.67 ± 0.16	195 ± 33	7.6 ± 0.2	130 ± 6.5
Endorem[b]	Dextran-stabilized maghemite crystals		72−100	30	100
Sinerem[c]	id		20	24	65

[a] From this work. [b] From ref 5. [c] From ref 29. [d] In mol of Fe(III) per mol of total lipid. [e] Mean hydrodynamic diameter from QELS. [f] From linear regression of the variation of the inverse of the relaxation time T_1 or T_2 versus Fe(III) concentration in the 10^{-2}−10 mM range (correlation coefficient higher than 0.98).

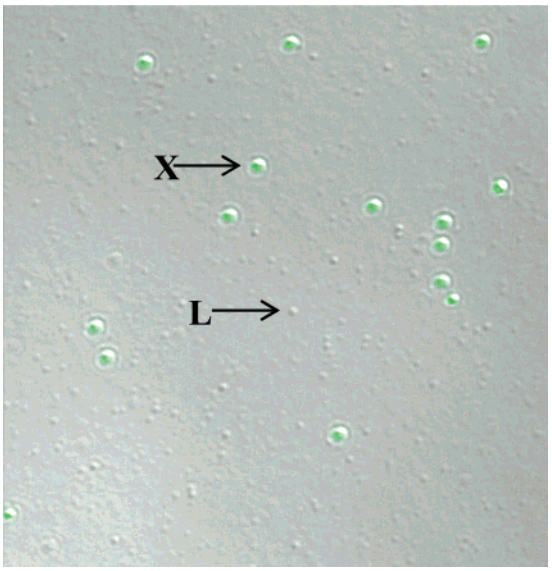

Figure 2. Superimposed confocal microscopy images of (L) EPC:DSPE-PEG_{2000} (95:5 mol %) MFL (Nomarski image, 0.2 mM total lipid concentration) and (X) 200 nm-beads of a fluorescent standard latex. Incident ion-laser wavelength: 488 nm.

of the vesicle unit diameter or to leakage of ferrofluid. Besides, 10^{-2} mM Fe(III) maghemite suspensions were highly stable in A and B media. In contrast, strong particle aggregation and precipitate formation occurred in biological medium C within 2 days.

Magnetic Properties. Magnetization curves recorded from free and liposome-encapsulated maghemite particles revealed superparamagnetic behavior without hysteresis. As seen in Figure 4, both curves presented the same shape, which was well fitted by Langevin's law for a log-normal distribution of magnetic grains of 7.7 nm mean diameter and 0.37 standard deviation.

Magnetophoresis of conventional and PEG-ylated MFL was performed at 20 °C in a specially designed chamber.[25] Both types of magnetic-fluid-loaded liposomes moved in an applied magnetic field gradient as clearly displayed by Figure 5. Taken together, these results proved that the intrinsic magnetic properties of the ferrofluid were preserved after encapsulation within liposomes.

The relaxometric properties of the initial maghemite suspension, conventional MFL, and three PEG-ylated MFL preparations encapsulating different local iron concentrations were studied. In every case, the variation of the inverse of the

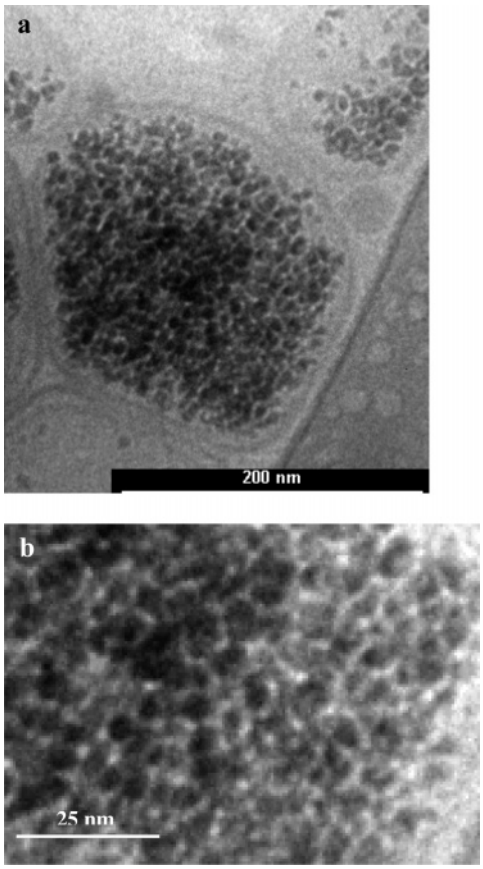

Figure 3. Cryo-TEM micrographs of EPC:DSPE-PEG_{2000} (95:5 mol %) MFL with 1.8 mol of ferrofluid loaded per mol of lipids. Total lipid concentration is equal to 1 mM. Picture (b) is an overview of picture (a) at a scale 4× larger and shows individual grains separated by a water layer.

relaxation times T_1^{-1} or T_2^{-1} versus Fe(III) concentrations was linear and the slopes evaluated as r_1 or r_2 relaxivities. These data are summarized in Table 1 and compared to those obtained under the same conditions for commercially available Endorem and Sinerem. First, whatever the magnetic colloid, either free iron oxide particles or loaded liposomes, transversal relaxivity r_2 was found to be significantly higher than longitudinal r_1, confirming the efficiency of these systems as T_2 contrast agents. Interestingly, MFL systems showed better efficiency, as shown by a significant increase in the r_2/r_1 ratio. This was systematically accompanied by a decrease of the r_1 value and an increase in the r_2 value as compared to the free ferrofluid. Moreover, in the case of PEG-ylated MFLs, these variations appeared

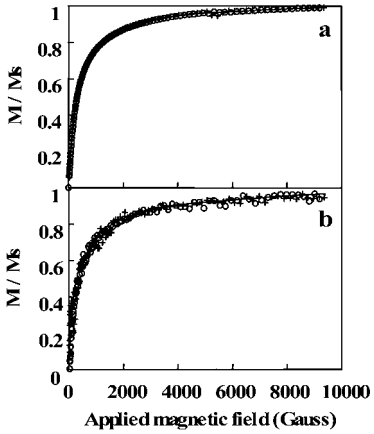

Figure 4. The variation of the magnetization normalized to the saturation magnetization (M/M_s) of (a) the ferrofluid ([Fe] = 50 mM) and (b) EPC:DSPE-PEG$_{2000}$ (95:5 mol %) MFL ([Fe] = 14.5 mM) as a function of applied magnetic field is well fitted by Langevin's law for a log-normal distribution of superparamagnetic grains of 7.7 nm in diameter and standard deviation of 0.37 (solid line). The + and ○ represent the field rise and field decrease, respectively.

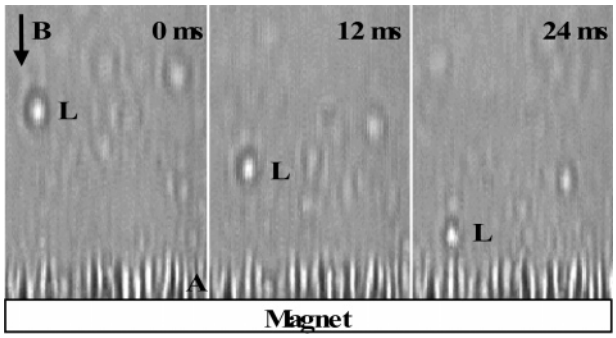

Figure 5. Evidence of the magnetophoretic mobility of EPC:DSPE-PEG$_{2000}$ (95:5 mol %) MFL submitted to a magnetic field gradient of 36 T m^{-1} (magnetic field B of 360 mT). Accumulation of the liposomes (L) aligned along the magnetic field lines (A). Time (ms) is indicated on the pictures. 0.8 cm along the arrow corresponds to an effective particle shifting of 30 μm along the magnetic field B.

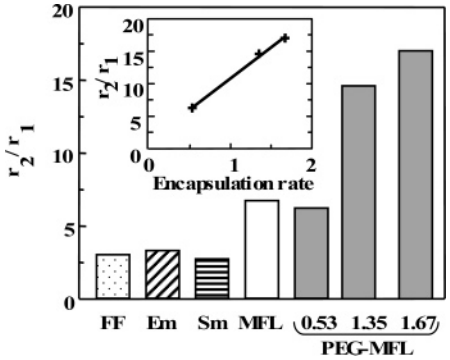

Figure 6. Ratios of transversal relaxivity r_2 to longitudinal relaxivity r_1 found at 0.47 T and 37 °C for free iron oxide particles (FF), EPC (100%) MFL (MFL) at iron loading of 0.35 mol of Fe(III) per mol of lipid and EPC:DSPE-PEG$_{2000}$ (95:5 mol %) MFL (PEG-MFL) at different iron loadings (indicated in Fe(III) to lipids molar ratios). Endorem (Em) from ref 5, Sinerem (Sm) from ref 29. Inset: variation of the ratio r_2/r_1 versus iron loading for PEG-ylated MFL (PEG-MFL).

proportional to the iron loading (Figure 6); that is, the higher was the iron content entrapped per liposome, the smaller was the r_1 value, and the higher were both the r_2 value and the r_2/r_1 ratio. The measurements made on conventional MFL with an iron loading of 35 mol % led to relaxivities r_1 and r_2 being

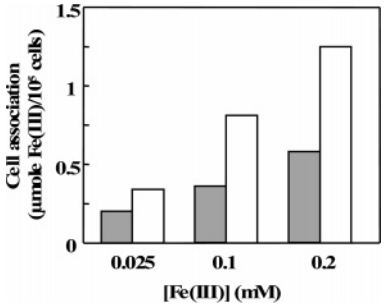

Figure 7. Association of EPC (100%) MFL (white bars) and EPC:DSPE-PEG$_{2000}$ (95:5 mol %) MFL (grey bars) with J774 macrophage-like cells after a 4 h-incubation at 37 °C as a function of the iron concentration in the incubation medium.

smaller than those measured for PEG-ylated MFL, but the contrast efficiency given by the r_2/r_1 ratio was comparable to that of PEG-ylated MFL with the closest iron loading of 53 mol % (Table 1).

In Vitro Experiments. Cytotoxicity. Viability of J774 cells after 4- and 24-h incubation with either free maghemite particles or MFL was followed as a function of iron concentration in the range 2×10^{-6} to 2 mM Fe(III). Unloaded liposomes used as controls showed no significant lipid cytotoxicity, in particular of the derivative DSPE-PEG$_{2000}$, at concentrations lower than 2 mM. Above this concentration, cell viability was reduced by 25% after a 24-h incubation. Loading of liposomes with ferrofluid did not result in any difference in cell survival, except for conventional MFL at concentrations higher than 0.2 mM lipids (0.2 mM Fe(III)), which reduced cell viability by 40% after 24 h. In contrast, free maghemite particles strongly affected J774 viability. After a 4-h incubation, the percentage of surviving cells was significantly lower than that found for liposomes and reached 50% at 2×10^{-2} mM Fe(III) and only 20% at 1 mM Fe(III). After 24 h, contact with the cell culture medium provoked the aggregation of the particles accompanied by the death of the cells, whatever the iron content (data not shown).

Cell Association. Cell association experiments were performed under nontoxic conditions, that is, lipids and Fe(III) concentrations not exceeding 0.66 and 0.55 mM, respectively. After a 4-h incubation of J774 cells in the presence of either conventional or PEG-ylated MFL, the amounts of iron associated with the cells were determined as a function of the amount of iron initially introduced into the culture medium. The results are illustrated in Figure 7. The presence of PEG chains grafted onto the surface of the liposomes reduced iron capture by the macrophages. On the basis of 0.2 mM Fe(III) encapsulated within MFLs, that is 0.56 mg of iron per 10^5 cells, cell-associated iron reached 67.2 μg per 10^5 cells for conventional liposomes as compared to half as much (28 μg per 10^5 cells) for PEG-ylated ones.

Magnetic Resonance Angiographic Imaging. The effect of PEG-ylated MFL on blood contrast in two different types of T_1-weighted sequences, either SE sequence or SPGR sequence, was measured as a function of time (Figure 8). Analysis of blood contrast on SE sequences as a function of time revealed that a strong negative enhancement is rapidly reached and is maintained for at least 5 h at −40% of enhancement as compared to untreated animals. 24 h after injection, PEG-ylated MFL reveal their T_1 effect with a positive enhancement that reached 20%.

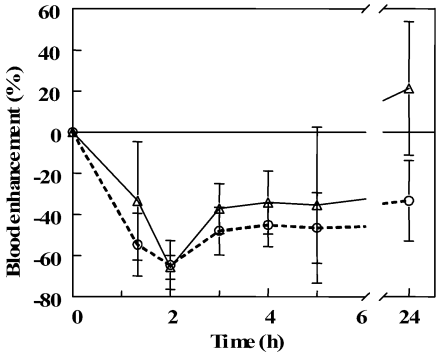

Figure 8. Blood contrast enhancement as a function of time and weighting in mice after intravenous injection of EPC:DSPE-PEG$_{2000}$ (95:5 mol %) MFL (7.2 mg/kg) at 20 mM total lipid and 25 mM iron concentrations. (△) SE sequences; (○) SPGR sequences.

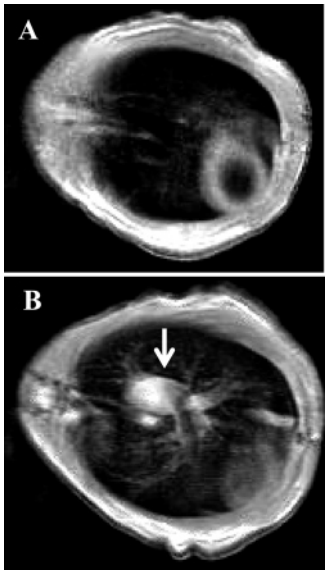

Figure 9. Axial T1-weighted spin−echo images (TR/TE 500/13) at the level of the upper thorax of a mouse, 24 h after injection of 7.2 mg/kg of (A) EPC (100 mol %) and (B) EPC:DSPE-PEG2000 (95:5 mol %) MFL at 20 mM total lipid and 25 mM iron concentrations. The strong enhancement of the pulmonary artery tronc (arrow) indicates persistent circulating liposomes.

Identical analyses were performed on SPGR images. A negative contrast enhancement was reached within 5 h after injection and maintained over 24 h at around −40%. Figure 9 shows a typical example of PEG-ylated MFL enhancement of MR images of vessels in mice. 24 h after intravenous injection of PEG-ylated MFL, they significantly brightened pulmonary arteries and small peripheral vessels with a contrast efficiency of 22% positive enhancement as compared to control animals. Similar experiments performed by injecting either free ferrofluid or loaded into conventional liposomes did not allow any visualization of the vessels after 24 h (data not shown).

Discussion

Our objective in this work was to provide a simple and reliable method for the preparation of magnetic-fluid-loaded liposomes combining physical and biological stability, efficient MRI contrast, and prolonged blood circulation time. The principle of this method could appear rather classic. It indeed consists of forming liposomes directly within the magnetic fluid so that some magnetic particles are trapped inside the vesicles while others remain outside. The major and really new trick of our method is to completely remove the external contaminating magnetic material without liposome dilution or damage. Many similar attempts have appeared in the liposome literature over the last 20 years,[3,9] but only few of them have actually succeeded and shown convincing results, which would allow applications in the fields of magnetic cell sorting,[30,31] magnetic drug targeting[32] or delivery,[33,34] hyperthermia,[35−37] or MRI.[38,39] This slow development can be explained principally by the difficulty of combining two separate colloids, the ferrofluid and the lipid vesicles, while preserving the structure and properties of each. Two strategies have been used to encapsulate ferrofluids within closed lipid bilayers and form what are usually called "magnetoliposomes". The first procedure consists of adsorbing lipids directly onto iron oxide beads with a 100% encapsulation efficiency. The advantages are the obtention of small particles not exceeding 50 nm in diameter, which are particularly resistant to solubilizing amphiphiles such as detergents.[37,40,41] However, the absence of internal aqueous compartments capable of retaining hydrosoluble material can be considered as a limitation for applications in drug delivery or targeting. The second procedure is the conventional encapsulation of iron oxide nanoparticles into large unilamellar liposomes (LUV). Here, optimization seeks the best compromise between loading, which should be as high as possible, and vesicle diameters, which should be small enough to allow systemic administration. Therefore, lipid hydration in the presence of the magnetic colloid followed by sequential extrusion appears to be a suitable method, leading to LUV of reproducible size and calibrated as a function of filters pore diameter.[42,43] We are able to produce 200−300 nm magnetic-fluid-loaded LUVs, intermediate between 100-nm sonicated magnetoliposomes[38] and micrometer-sized ones prepared by reverse phase evaporation[32,44] or freeze−thawing.[31] Whatever the method, some nonencapsulated ferrofluid always remains in the dispersion, and this has to be removed to better control and often significantly improve the efficiency of the magnetoliposomes. Three purification techniques can be employed, centrifugation,[31,32,41,45] magnetic sorting,[40,44] and GEC.[18,46] The last is undoubtedly the simplest at the laboratory scale, and in this work we have found conditions that avoid dilution of

(29) Jung, C. W. *Magn. Reson. Imaging* **1995**, *13*, 675−691.
(30) Margolis, L. B.; Namiot, V. A.; Kliukin, L. M. *Biofizika* **1983**, *28*, 884−885.
(31) Domingo, J. C.; Mercadal, M.; Petriz, J.; De Madariaga, M. A. *J. Microencapsulation* **2001**, *18*, 41−54.
(32) Viroonchatapan, E.; Ueno, M.; Sato, H.; Adachi, I.; Nagae, H.; Tazawa, K.; Horikoshi, I. *Pharm. Res.* **1995**, *12*, 1176−1183.
(33) Viroonchatapan, E.; Sato, H.; Ueno, M.; Adachi, I.; Murata, J.; Saiki, I.; Tazawa, K.; Horikoshi, I. *J. Drug Targeting* **1998**, *5*, 379−390.
(34) Babincova, M.; Leszczynska, D.; Sourivong, P.; Babinec, P. *Cell. Mol. Biol. Lett.* **1999**, *4*, 625−630.
(35) Le, B.; M., S.; Kitade, T.; Honda, H.; Yoshida, J.; T., W.; Kobayashi, T. *J. Chem. Eng. Jpn.* **2001**, *34*, 66−72.
(36) Hamaguchi, S.; Tohnai, I.; Ito, A.; Mitsudo, K.; Shigetomi, T.; Ito, M.; Honda, H.; Kobayashi, T.; Ueda, M. *Cancer Sci.* **2003**, *94*, 834−839.
(37) Ito, A.; Kuga, Y.; Honda, H.; Kikkawa, H.; Horiuchi, A.; Watanabe, Y.; Kobayashi, T. *Cancer Lett.* **2004**, *212*, 167−175.
(38) Pauser, S.; Reszka, R.; Wagner, S.; Wolf, K. J.; Buhr, H. J.; Berger, G. *Anti-Cancer Drug Des.* **1997**, *12*, 125−135.
(39) Bulte, J. W. M.; Cuyper, M. d.; Despres, D.; Frank, J. A. *J. Magn. Magn. Mater.* **1999**, *194*, 204−209.
(40) De Cuyper, M.; Joniau, M. *Eur. Biophys. J.* **1988**, *15*, 311−319.
(41) Shinkai, M.; Suzuki, M.; Iijima, S.; Kobayashi, T. *Biotechnol. Appl. Biochem.* **1994**, *21*, 125−137.
(42) Lesieur, S.; Grabielle-Madelmont, C.; Paternostre, M. T.; Ollivon, M. *Anal. Biochem.* **1991**, *192*, 334−343.
(43) Szoka, F., Jr.; Papahadjopoulos, D. *Annu. Rev. Biophys. Bioeng.* **1980**, *9*, 467−508.
(44) Elmi, M. M.; Sarbolouki, M. N. *Int. J. Pharm.* **2001**, *215*, 45−50.
(45) Babincova, M. *Bioelectrochem. Bioenerg.* **1993**, *32*, 197−189.
(46) Kuznetsov, A. A.; Filippov, V. I.; Alyautdin, R. N.; Torshina, N. L.; Kuznetsov, O. A. *J. Magn. Magn. Mater.* **2001**, *225*, 95−100.

the dispersion and ensure high magnetoliposome purity. Also, we have reached a very satisfactory loading of about 1.7 mol of iron per mol of lipids as compared to data already reported for LUVs of 1.5 mol of iron per mol of lipids.[31] On the basis of the average iron content of maghemite particles (close to 38 iron atoms per nm^3),[25] an estimate of the mean number n_{mp} of magnetic particles of volume V_{mp} (nm^3) per liposome of radius R can be calculated according to $n_{mp} = rA/(V_{mp}\cdot 38)$, where r is the iron loading (mol of iron per mol of lipids) and A is the number of lipid molecules per liposome. A is given by: $A = (4\pi/3)R^2e(d/M)N$, where e is the average bilayer thickness ($e \approx 35$ Å for a PEG-ylated phospholipid bilayer[22]), d is the specific mass of the lipid ($d \approx 10^6$ g m^{-3}), M is their average molar mass ($M = 0.95M_{EPC} + 0.05M_{DSPE-PEG} = 862$ g mol^{-1}), and N is Avogadro's number. One PEG-ylated MFL of radius 100 nm with 1.7 mol/mol iron loading then entraps about 60 magnetic particles on average.

There are other difficulties involved in developing a liposomal carrier for ferrofluids for in-vivo use. The first is to prevent physical instability of the magnetic fluid from in physiological media (at neutral pH and ionic strength equivalent to about 300 mosmol) while liposomes are being formed. In this work, we choose to stabilize the maghemite-based colloid by electrostatic repulsion of the nanocrystals through surface coating with negatively charged citrate anions. In particular, the association of the citrate anions with the Fe(III) iron oxide is stable on dilution in NaCl solutions, allowing the transfer of the particles into isotonic media in the same way as polymer-coated ones. Under these conditions, the unit size and monodisperse state of the magnetic grains can be preserved during liposome extrusion and GEC purification as clearly shown by cryo-TEM (Figure 3) and by QELS measurements performed on fractions collected after GEC (Figure 1c). The very narrow size distribution and the magnetic diameter of 7.7 nm are usual characteristics of maghemite nanoparticles.[47] The larger size found by QELS may be explained by the fact that the hydrodynamic diameter takes into account the layer of water molecules carried by the particles during their Brownian motion. Interestingly, citrate-stabilization does not generate any specific interactions between the magnetic fluid and phospholipids, either PEG-ylated or not, in contrast to dextran-coating which provokes liposome aggregation.[34,48,49] The important consequence of these results is that liposome-encapsulation preserves the native superparamagnetic behavior of the ferrofluid, as demonstrated by the superimposition of magnetization curves from maghemite particles before and after encapsulation.

Citrate-stabilization of the ferrofluid was not efficient in biological media. On contact with cell culture RPMI medium supplemented with serum, maghemite particles aggregate rapidly to form an iron oxide deposit, which is at the origin of the apparent ferrofluid toxicity toward the J774 cells. Other studies have previously demonstrated that iron oxide particles forming ferrofluids were quite nontoxic, providing they were prevented from aggregation by adding sodium citrate to the cell-culture medium and in the absence of serum.[25,50,51] Aggregation may be due to competition between citrate anions and serum proteins for adsorption onto the particles, which would change the net charge of their surface, or to the presence of positively charged species, which would catalyze their flocculation. Liposome-encapsulation totally resolves this problem as it avoids direct interaction of the ferrofluid with external medium. Therefore, the MFLs appeared serum-compatible, encouraging their use in vivo.

Another interesting result that could be deduced from the cell-association experiments concerned the efficiency of the macrophages to uptake ferrofluid. 4-h incubation of cells with conventional MFL containing 0.2 mM iron oxide led to around 6.7 pg of iron per cell. This is equivalent to the results previously obtained with incubation in the presence of 0.5 mM free maghemite particles stabilized by dimercaptosuccinic acid.[51] On the basis of iron content of the incubation medium, conventional liposomes favor thus free particles to ferrofluid cell-association. In contrast, PEG-ylated MFLs led to only 2.8 pg of iron per cell and hinder cell-association as compared to the action of free ferrofluid.

The second major obstacle to the use of liposomes as drug delivery systems is the rapid removal of conventional formulations from circulation by the cells of the mononuclear phagocyte system (MPS, reticuloendothelial system). To restrict this, we have opted for the extensively documented strategy of grafting PEG moieties onto the liposome surface.[14,23,52−54] Curiously, this approach has not been widely investigated in the case of magnetoliposomes despite several encouraging reports.[31,38,55] Hydrophilic polymer chains exert steric repulsion on any approaching molecule or particle. Hence, liposomes are prevented from aggregation and fusion processes, their destabilization by amphiphilic compounds is delayed, and the adsorption of proteins leading to recognition by the MPS is strongly hindered. Our results demonstrate that incorporation of 5 mol % of DSPE-PEG_{2000} into the membrane of EPC LUVs produces magnetic-fluid-loaded liposomes of high physical stability without added toxicity toward cells. Moreover, in vitro experiments have undoubtedly showed that their association with macrophages is reduced by a factor of about 2 as compared to conventional magnetoliposomes. This evidence of steric stabilization obtained in vitro has furthermore been confirmed in vivo by direct MR imaging of the magnetic-fluid-loaded PEG-ylated LUVs within mouse vessels over 24 h after intravenous injection (Figure 9). It is highly probable that the ferrofluid visualized by MRI is still entrapped within intact liposomes because free maghemite particles do not exhibit such longer circulation times.[56] Moreover, no contrast enhancement was observed 24 h after administration of conventional MFL (Figure 9A), supporting that the presence of PEG chains on the liposome surface was necessary to maintain circulation in blood over a 24-h period of time.

(47) Halbreich, A.; Roger, J.; Pons, J. N.; Geldwerth, D.; Da Silva, M. F.; Roudier, M.; Bacri, J. C. *Biochimie* **1998**, *80*, 379−390.
(48) Bogdanov, A. A., Jr.; Martin, C.; Weissleder, R.; Brady, T. J. *Biochim. Biophys. Acta* **1994**, *1193*, 212−218.
(49) Viroonchatapan, E.; Sato, H.; Ueno, M.; Adachi, I.; Tazawa, K.; Horikoshi, I. *J. Controlled Release* **1997**, *46*, 263−271.
(50) Wilhelm, C.; Gazeau, F.; Roger, J.; Pons, J. N.; Billotey, C.; Bacri, J. C. *Langmuir* **2002**, *18*, 8148−8155.
(51) Billotey, C.; Wilhelm, C.; Devaud, M.; Bacri, J. C.; Bittoun, J.; Gazeau, F. *Magn. Reson. Med.* **2003**, *49*, 646−654.
(52) Allen, T. M.; Hansen, C.; Martin, F.; Redemann, C.; Yau-Young, A. *Biochim. Biophys. Acta* **1991**, *1066*, 29−36.
(53) Allen, T. M.; Moase, E. H. *Adv. Drug Delivery Rev.* **1996**, *21*, 117−133.
(54) Papahadjopoulos, D.; Allen, T. M.; Gabizon, A.; Mayhew, E.; Matthay, K.; Huang, S. K.; Lee, K. D.; Woodle, M. C.; Lasic, D. D.; Redemann, C.; et al. *Proc. Natl. Acad. Sci. U.S.A.* **1991**, *88*, 11460−11464.
(55) Hodenius, M.; De Cuyper, M.; Desender, L.; Muller-Schulte, D.; Steigel, A.; Lueken, H. *Chem. Phys. Lipids* **2002**, *120*, 75−85.
(56) Chouly, C.; Pouliquen, D.; Lucet, I.; Jeune, J. J.; Jallet, P. *J. Microencapsulation* **1996**, *13*, 245−255.

The efficacy of a MR contrast agent is commonly evaluated in terms of its relaxivities r_1 and r_2 defined as the rates at which the excited solvent nuclei (protons) relax to regain their initial equilibrium state. They are determined from the linear relationship $1/T_{i,obs} = 1/T_{i,dw} + r_i$ [A] (measured ^{1}H relaxation time, $T_{i,obs}$; water diamagnetic constant, $T_{i,dw}$; contrast agent concentration, [A]) and are then expressed in s^{-1} per contrast agent concentration. Relaxivity r_1 is related to the spin−lattice relaxation process, the excited nuclei giving off their energy to the surrounding environment. Relaxivity r_2 characterizes the spin−spin relaxation process through which an excited nucleus exchanges its energy with a low-energy one. MR contrast results from the difference between r_1 and r_2 values. In the case of T_2-agents, which accelerate the spin−spin relaxation process, the higher is the r_2 to r_1 ratio, the better is the agent's effectiveness. In this respect, the data in Table 1 show that encapsulation of the maghemite particles within liposomes concomitantly increases r_2 and decreases r_1, thus significantly improving the MR contrast ability of the ferrofluid. Moreover, the higher is the internal Fe(III) concentration, the better is the contrast obtained with ferrofluid-loaded liposomes. This behavior has been routinely observed when lipid vesicles are used as reservoirs of T_2 contrast agents. Indeed, the efficiency of T_2 contrast agents mainly arises from their local concentration, which should be high (spin−spin relaxation mechanism) and preserved by their encapsulation within liposomes. The behavior of T_1 contrast agents, such as those based on gadolinium,[13,57,58] conversely requires a direct contact with the water molecules of the tissues (spin−lattice relaxation mechanism) to be efficient, so that it is preferable to bind them to the external surface of the carrier. Relaxation processes in the presence of encapsulated systems are complex, and their explanation is out of the scope of this study. Nevertheless, our experimental findings agree with the theoretical background discussed previously.[3,4] The gain obtained with liposomes mainly arises from the clustering effect they exert at two levels. On one hand, entrapping within vesicles maintains high local concentrations of the magnetic fluid whatever the dilution factor applied to the magnetoliposomes. On the other hand, closed vesicles create a separate aqueous compartment where the water molecules are confined, and which is distinct from the external aqueous continuum. The lipid bilayer that forms the vesicle membrane acts as a barrier to the exchange of the water molecules between the interior and the exterior of the liposomes. As the ferrofluid is contained only in the interior, the first consequence is that spin−lattice relaxation is kinetically limited by the diffusion rate of water through the lipid bilayer.[3,57] Our results confirm this effect because the r_1 value is decreased by at least a factor of 2 when the maghemite particles are encapsulated into liposomes. Furthermore, we have found that the higher is the Fe(III) concentration, the smaller is the relaxivity r_1. This result has been already obtained for iron oxide particles confined within cells.[51] It has been explained not only by the lowering of the proton exchange between interior and exterior of the cell but also and especially by the saturation of the relaxing effect due to the confined ferrofluid. In good agreement with the data in Table 1, it has been verified that in the presence of an external magnetic field, ferrofluid-loaded vesicles cause distortions and fluctuations in the external field, which contribute to shortening the transverse relaxation time and enhancing the r_2 value.[3,59] Moreover, these data show that for given vesicle lipid composition, size, and number, the predominance of spin−spin relaxation is emphasized by increasing maghemite content in the liposomes. Finally, the combination of reduced r_1 and enhanced r_2 raises the relaxivity ratio r_2/r_1 up to 17, about 6 times higher than the value reached by the free ferrofluid. Interestingly, PEG-ylated liposomes loaded at 10.6 mM Fe(III) show nearly the same r_2/r_1 ratio as that of conventional EPC liposomes at 7 mM Fe(III) (Table 1). This may arise from the difference in vesicle mean diameter, larger vesicles privileging better magnetic susceptibility,[58] but also from the presence of hydrophilic PEG chains on the surface and inside the liposomes, which could modify the water state in the vicinity of the iron oxide particles as compared to a homogeneous EPC bilayer.[60]

The influence of PEG-ylated MFL on blood contrast was studied as a function of time. During the first 5 h after MFL injection, blood contrast was clearly dark, revealing the predominance of T_2 effect of PEG-ylated MFL, independently of the sequence. Such T_2 behavior of the ferrofluid could not be achieved unless it was present at high local concentration. This strongly suggested that, at this time, a notable proportion of the PEG-ylated MFL remained both intact and circulating. After 24 h, the MFLs gave T_1-weighted brightened images of pulmonary arteries and surrounding vessels according to SE sequence. This means that PEG-ylated MFLs were still present in the blood flow. However, in agreement with theoretical background,[61] this implies the dilution of the contrast agent. This arose rather from the partial elimination of the liposomes without affecting their content than from leakage of part of the magnetic fluid. Indeed, the preserving of the ferrofluid loading within the liposomes was shown by the contrast analysis of the SPGR sequences (Figure 8). Whereas positive blood enhancement was obtained from SE sequences (+22%), the strong negative enhancement of blood measured immediately after injection of PEG-ylated MFLs was globally maintained up to 24 h at around −40%. SE sequences report T_1-related contrast and then reveal positive enhancement, whereas SPGR sequences are acutely sensitive to T_2 effect so that they report negative enhancement of blood even at low concentrations of T_2 contrast agents.[61] Therefore, the variation of the blood contrast over time could be attributed to the slow elimination of the MFLs from the blood compartment rather than to a progressive release of the maghemite particles from the liposomes.

Conclusion

In conclusion, this study describes an optimized and very simple procedure to prepare 200 nm unilamellar liposomes sterically stabilized by PEG chains and containing superparamagnetic maghemite particles whose concentration can be varied. The MFLs are highly stable both in vitro and in vivo, nontoxic, and present long-circulating behavior in blood. Their magnetic properties rank them among efficient MR T_2 contrast

(57) Fossheim, S. L.; Fahlvik, A. K.; Klaveness, J.; Muller, R. N. *Magn. Reson. Imaging* **1999**, *17*, 83−89.
(58) Glogard, C.; Stensrud, G.; Hovland, R.; Fossheim, S. L.; Klaveness, J. *Int. J. Pharm.* **2002**, *233*, 131−140.
(59) Pouliquen, D.; Perroud, H.; Calza, F.; Jallet, P.; Le Jeune, J. J. *Magn. Reson. Med.* **1992**, *24*, 75−84.
(60) Trubetskoy, V. S.; Cannillo, J. A.; Milshtein, A.; Wolf, G. L.; Torchilin, V. P. *Magn. Reson. Imaging* **1995**, *13*, 31−37.
(61) Clement, O.; Siauve, N.; Cuenod, C. A.; Vuillemin-Bodaghi, V.; Leconte, I.; Frija, G. *J. Comput. Assist. Tomogr.* **1999**, *23 Suppl 1*, S45−52.

agents. The first MRI experiments performed here demonstrate their potential for in vivo imaging. The sum of these results encourages further investigations of MFL applications from diagnostic to therapeutics. MFLs indeed appear good candidates for the delivery of drugs, which should be incorporated into the lipid bilayer or encapsulated in the internal volume of their vesicle structure. The entrapped ferrofluid can serve as MR diagnostic agent to follow the drug carrier or be used for magnetic targeting or hyperthermia.[35] Studies concerning magnetic targeting of MFLs in solid tumors are currently being undertaken.

Acknowledgment. The electron microscopy was performed by J. P. Lechaire and G. Frébourg (UMR CNRS 7138 SAE) (Plateau technique-IFR83 CNRS-Biologie Intégrative-Université P.et M. Curie-Paris VI). We thank D. Talbot for iron dosage and V. Nicolas (Plateau Technique − Imagerie Cellulaire IFR75) for technical assistance and realization of the confocal studies. We thank M. Appel for her assistance during culture cells experiments. Finally, we thank Pr J. Bittoun, C. Vayssettes, and J. Prudhomme for their assistance with MRI. This work was supported by a grant of the Ministry of Research in France, by CNRS and ACI NR 145 (ACI Nanoscience et Nanotechnologie et Programme Interdisciplinaire Imagerie du Petit Animal).

JA0516460